MR. GRIFFIN LENTSCH (Orcid ID : 0000-0003-2465-9937)
DR. ANAND GANESAN (Orcid ID : 0000-0003-4944-9274)

DR. MANOJ MISRA (Orcid ID : 0000-0001-7895-8882)

Article type : Original Article

Manuscript Category: Experimental therapeutics / Preclinical (ETP)

TITLE PAGE

Article Type: Original Article

Title: *In vivo* multiphoton microscopy imaging of melasma

Griffin Lentsch[1], Mihaela Balu[1], Joshua Williams[1], Sanghoon Lee[1,2], Ronald M. Harris[3], Karsten König[4], Anand Ganesan[3], Bruce J. Tromberg[1], Nirmala Nair[5], Uma Santhanam[6], Manoj Misra[6]

[1]University of California, Irvine, Beckman Laser Institute, Laser Microbeam and Medical Program, Irvine, CA, 92612

[2]Department of Dermatology, Soonchunhyang University, Seoul, The Republic of Korea

[3]Department of Dermatology, University of California, Irvine

[4]Jenlab, GmbH, Jena, Germany

[5]Unilever R&D, Bangalore, India

[6]Unilever R&D, 40 Merritt Blvd, Trumbull, CT, 06611

Corresponding author: Manoj Misra, 40 Merritt Blvd, Trumbull, CT 06611, (203) 381-5743; fax: (203) 381-5497, Manoj.Misra@unilever.com

Conflicts of Interest: K. Koenig is the co-founder of Jenlab, GmbH. B.J. Tromberg and M. Balu report a pending patent, which is owned by the University of California, that is related to the technology described in this study. The Institutional Review Board and Conflict of Interest Office of the University of California, Irvine, have reviewed patent disclosures and did not find any concerns. No potential conflicts of interest were disclosed by the other authors.

SUMMARY/ABSTRACT

Melasma is a skin disorder characterized by hyperpigmented patches due to increased melanin production and deposition. In this pilot study we evaluate the potential of multiphoton microscopy (MPM) to characterize non-invasively the melanin content, location, and distribution in melasma and assess the elastosis severity. We employed a clinical MPM tomograph to image *in-vivo* morphological features in melasma lesions and adjacent normal skin in 12 patients. We imaged dermal melanophages in most dermal melasma lesions and occasionally in epidermal melasma. The melanin volume fraction values measured in epidermal melasma (14±4%) were significantly higher ($p<0.05$) than the values measured in peri-lesional skin (11±3%). The basal keratinocytes of melasma and perilesions showed different melanin distribution. Elastosis was predominantly more severe in lesions than in perilesions and was associated with changes in melanin distribution of the basal keratinocytes. These results demonstrate that MPM may be a non-invasive imaging tool for characterizing melasma.

SIGNIFICANCE

Identifying the depth of excess pigment is critical for successful treatment of melasma. Multiphoton microscopy demonstrates the ability to visualize non-invasively the melanophages, a sign of a prior inflammatory response, key in the differential diagnosis of melasma. Patients with melasma may be diagnosed more accurately using a rapid, label-free, non-invasive microscopy technique.

KEYWORDS

in vivo imaging; microscopy; melasma

INTRODUCTION

Melasma is a hyperpigmentary skin disorder characterized by irregular light to dark brown macules frequently found on the sun-exposed areas of the face, due to increased melanin production and deposition. Identifying the depth of excess pigment (epidermal and/or dermal) is critical for successful treatment. To date, there is no reliable method to determine the depth of melanin pigment, a key factor among others that make the treatment of melasma a difficult challenge. Biopsy is not commonly an option due to cosmetic reasons, and a heterogeneous melanin distribution is often present, which would require multiple sampling sites. Both a dermatoscope, and a Woods lamp (a light source based on UV illumination) are commonly used by dermatologists for melasma diagnosis as non-invasive alternatives to biopsy (Gilchrest et al., 1977; Sonthalia et al., 2017). However, several studies have shown that Wood's lamp examination is not accurate in determining the depth of melanin pigment(Grimes et al., 2005) and cannot predict treatment response(Lawrence et al., 1997).

Recent advances in optical imaging technologies hold the potential to improve the accuracy of melasma diagnosis and impact its treatment. Reflectance confocal microscopy (RCM) is a laser scanning microscopy technique that derives its contrast from variations of tissue refractive index, providing gray scale images with sub-micron resolution. Generally, gray scale images are sufficient for the overall assessment of tissue structure. Therefore, RCM was employed in several studies for imaging melasma (Sgouros et al., 2014). Findings included increased pigmentation of the epidermis in melasma lesions compared to adjacent normal skin, as well as presence of melanophages in pigmented lesions diagnosed by histopathology as dermal/mixed melasma(Kang et al., 2010; Liu et al., 2011). RCM was also evaluated as a potential imaging tool for monitoring treatment efficacy of melasma(Ardigo et al., 2010; *Goberdhan* et al., 2013; Longo et al., 2014).

Multiphoton microscopy (MPM) is a more complex laser-scanning microscopy technique compared to RCM. It provides sub-micron resolution images of living tissues in their native environment with contrast from two-photon excited fluorescence (TPEF) and second harmonic generation (SHG). In skin tissue, TPEF signal is generated by reduced nicotinamide adenine dinucleotide (NADH), flavin adenine dinucleotide (FAD), keratin, melanin, and elastin fibers, while SHG signal is generated by collagen fibers. MPM involves a more complex technology compared to RCM, the TPEF and SHG signals provide enhanced contrast, facilitate image interpretation, allow evaluation of elastosis and development of quantitative analysis strategies based on MPM molecular contrast as recently shown by our group and others(Balu et al., 2014; Bradley and Roth, 2007; Saager et al., 2015).

In this pilot study, we evaluate the potential of MPM imaging to characterize the melanin content, location, and distribution in melasma and assess the elastosis severity, a feature that has been suggested to be related to melasma (Hernández-Barrera et al., 2008; Kang et al., 2002; Sarvjot et al.,

2009). We discuss potential relationships between melanin distribution, presence of melanophages and elastosis.

MATERIALS & METHODS

Study Design

The experiments were conducted with the full consent of each subject using a protocol approved by the Internal Review Board for clinical research in human subjects at the UC Irvine.

Twelve female subjects age 29-58 and Fitzpatrick skin type II-IV with facial melasma lesions were enrolled in this pilot study. Board certified dermatologists A.G. and S.L used a Woods lamp to determine melasma diagnosis. Seven subjects were diagnosed with primarily epidermal melasma and five were diagnosed with primarily dermal or mixed. Four subjects had a history of treatment for their melasma within the past year.

All melasma lesions were located on the face mainly on cheek and forehead. Imaging sites included melasma and perilesional areas. Perilesional areas were located within a few centimeters from the lesion. Multiple locations at each site were imaged *in vivo* using MPM.

Data acquisition

For in vivo imaging of melasma, we employed an MPM-based clinical tomograph (MPTflex, JenLab GmbH, Jena, Germany) described in detail in prior studies(Balu et al., 2014; Balu et al., 2017; Balu et al., 2015b).

We acquired data using two excitation wavelengths, 790nm and 880nm. The 790nm shows the overall morphology through emission signals from all fluorophores (NADH/FAD, keratin, melanin, elastin fibers) and collagen fibers in skin (Fig. 1 A). The 880nm was used in order to maximize the melanin contrast against TPEF signals from other components of the epidermis (keratin, NADH/FAD), which facilitates quantification of melanin in the epidermis (Fig. 1 B). For both wavelengths, the TPEF signal was detected over the spectral range of 410 to 650 nm, whereas the SHG signal was detected over a narrow spectral bandwidth of 385 to 405 nm through emission filters placed in the TPEF and SHG detection channels, respectively. We used a Zeiss objective (40X, 1.3 NA, oil immersion) for focusing into the tissue. The power used at the sample was a few mW (epidermis) and was gradually increased with depth up to 30 mW (dermis), below the estimated skin tissue damage thresholds(Fischer et al., 2008; Masters et al., 2004).

We acquired optical sections of 200x200μm^2 at different depths ranging from 0 to about 150μm (5μm steps). Since each optical section is limited to a small scan field, to improve the overall characterization of the examined skin we acquired three stacks of images for each of the lesional and perilesional areas and for each excitation wavelength, 790nm and 880nm, a total of twelve stacks for each subject.

Data analysis

Assessment of melanophages

The presence/absence of dermal melanophages in MPM images was determined by R.M.H based on visual assessment. Criteria for identification of melanophages included large size (>12 μm diameter)(Guitera et al., 2010; Ochoa et al., 2008), increased fluorescence brightness compared to fluorescence from surrounding elastin fibers(Majdzadeh et al., 2015), presence of a nucleus, shape, ill-defined cytoplasmic borders, and clustering distribution within the dermis(Pellacani et al., 2008).

Assessment of epidermal melanin content

For measuring the melanin volume fraction (MVF), we used the TPEF images acquired in the lesional and perilesional epidermal areas (880 nm excitation wavelength). The MVF corresponding to each acquired stack was calculated following image processing based on an algorithm described in a previous study(Saager et al., 2015). In short, each TPEF image was converted into a binary image using the same threshold for all images. The pixels of value "1" represented the melanin contribution and were used to calculate the area occupied by melanin in each image and subsequently, the volume occupied by melanin in each acquired stack (Fig. 1 C). The MVF was defined as the ratio between the melanin volume and the imaged volume.

Assessment of elastosis

The severity of solar elastosis (overproduction or clumping of elastin in the dermis)(Braverman and Fonferko, 1982) in the lesional and perilesional areas was evaluated semi-quantitatively as "mild", "moderate" and "severe", based on visual assessment, by the board certified dermatologist R.M.H who has extensive expertise with MPM image interpretation from his involvement in previous studies on MPM clinical skin imaging.(Balu et al., 2014; Balu et al., 2015b; Pouli et al., 2016) We correlated this evaluation with a more rigorous quantitative assessment based

on the TPEF and SHG signals from elastin and collagen fibers, respectively. For each patient, we selected about 5 frames corresponding to superficial dermis in each stack. We measured the mean intensity of the TPEF signal from elastin fibers and of the SHG signal from collagen fibers in each frame. We determined the elastosis severity in the superficial dermis by defining a metric as a/(a+b), where a and b represented the mean intensity of the TPEF and SHG signals, respectively. Based on its definition, this metric increased with the increase of elastosis. We used a pair t-test to determine whether the metric value was significantly different in the lesion from perilesion of each patient.

RESULTS

We analyzed the MPM images acquired *in vivo* from melasma lesional and perilesional skin in 12 subjects. There were three parameters of interest in the evaluation of melasma: the presence of dermal melanophages, epidermal melanin content and distribution, and elastosis severity. We assessed these parameters in both melasma (lesion) and adjacent normal skin (perilesion) for comparison purposes. We compared the quantitative parameters measured in two groups: epidermal and dermal/mixed melasma as diagnosed by the board certified dermatologists A.G. and S.L. based on Woods lamp. The following sections expand on the findings related to measured parameters.

Assessment of melanophages

The dermal melanophages we imaged could be classified in 4 groups: (1) clusters of small melanophages (10-15μm) (Fig. 2A), (2) clusters of large melanophages (15-20μm) (Fig. 2B), (3) dendritic melanophages (Fig. 2C), and (4) individual (scattered) melanophages (Fig. 2D). Table 1 includes the number of melanophages identified in the volume measured for each subject.

We imaged occasional dermal melanophages in one of the seven subjects diagnosed with epidermal melasma and larger number of melanophages (7-20) in four of the five subjects diagnosed with dermal/mixed melasma. In two of the subjects diagnosed with dermal melasma a small number of melanophages (4-12) were identified in the perilesion.

Assessment of epidermal melanin content and distribution

The melanin appears in the MPM images as bright fluorescence spots in the cellular cytoplasm, representing aggregates of melanosomes. The MPM images provided information about the melanin content and distribution in melasma compared to adjacent normal skin

Subjects in the epidermal melasma diagnosis group generally showed significantly ($p=0.03$) higher pigment amount in lesional skin (14±4%) compared to perilesional skin (11±3%) in the epidermis, while subjects diagnosed with dermal/mixed melasma presented similar pigment amount ($p=0.32$) in lesional skin (11±5%) compared to perilesional skin (13±6%) in the epidermis (Fig. 3).

Besides the difference in melanin amount, the lesions and perilesions also showed difference in melanin distribution. Pigment within the basal cells was distributed either towards the cellular membrane, away from the nucleus (Fig. 4A) or towards the nuclear membrane as melanin caps (Fig. 4B). Melasma was more often characterized by the melanin distribution towards the cellular membrane compared to adjacent normal skin. In melasma lesions, melanin caps were either absent or very few compared to adjacent normal skin. The MPM images shown in Figure 4 a, b, and their corresponding stacks shown in Figure 4 c, d, correspond to the 790 nm excitation. Melanin is visualized as bright fluorescence signal at this excitation wavelength. While images acquired at 880 nm excitation wavelength were used for estimating the melanin content (see example shown in Figure 1), the images acquired at 790 nm allow visualization of the dermal-epidermal junction and accurate identification of the basal layer through the SHG signal from the tops of the dermal papillae (Figure 4 c, d). Conversely, the fixed settings for the emission filters do not allow the separation of the TPEF and SHG signals for the 880 nm excitation (see Data Acquisition in Materials and Methods).

Assessment of elastosis

Elastosis was visualized by MPM as an over-production of normal elastin fibers (Fig. 5, A1, C1) or thickened, clumped elastin fibers (Fig. 5, B1, C2). The severity of elastosis in the lesional and perilesional areas was categorized semi-quantitatively as “mild,” “moderate,” or “severe” by the board-certified dermatologist R.M.H. Generally, MPM images of lesional skin showed an increase in elastosis severity compared to perilesional skin. Occasionally, perilesional normal skin showed increased elastosis compared to the adjacent melasma lesion as illustrated in Fig. 5 C1-C2. The dermatopathologist evaluation of elastosis was validated by employing a quantitative analysis based on the TPEF and SHG signals from elastin and collagen fibers, respectively. The parameter we used to determine the elastosis severity in the superficial dermis was defined as $a/(a+b)$, where a and b represented the mean intensities of the TPEF and SHG signals, respectively (see Methods). The value of this parameter ranged between 0.2 and 0.7 for both lesion and perilesion. Based on its definition, the parameter increased with the severity of elastosis. Thus, eight out of twelve subjects showed a significant increase in elastosis severity in their melasma area compared to perilesional skin ($p<0.05$), two subjects showed a significant increase in elastosis severity in their perilesional normal skin compared to melasma ($p<0.05$), while two other subjects showed a similar degree of elastosis severity in both lesion and perilesion.

Analysis of the lesional and perilesional dermal appearance and the corresponding epidermal melanin distribution revealed an interesting observation: 70% of lesions and perilesions showed increased elastosis and presence of melanophages associated with lack of melanin caps in the basal layer of the epidermis. This observation is illustrated by representative images in Figures 6 and 7.

DISCUSSION

This pilot study evaluated the potential of MPM to be used as a non-invasive imaging tool for visualizing melasma features, particularly melanophages, as a sign of prior inflammation, and for advancing our understanding of morphological changes related to this skin condition.

The most relevant feature we sought to capture by MPM imaging was the sign of a prior inflammatory response in the form of melanophages. Identification of melanophages in the dermis represents an indication of dermal pigment presence, a key element for differential diagnosis of melasma and successful treatment. MPM identified presence of melanophages in four out of five dermal/mixed melasma lesions and in two out of seven epidermal melasma lesions. Melanophages were also visualized in normal perilesional area of one patient diagnosed with epidermal melasma, and one patient diagnosed with dermal/mixed melasma. Presence of dermal melanophages in the epidermal melasma lesion indicates a potential erroneous clinical diagnosis of the lesion. The absence of melanophages in one dermal/mixed melasma is related to either an erroneous diagnosis of the lesion or very likely to the sampling limitation of MPM. Melanophages in dermal/mixed melasma lesions have been previously identified non-invasively by RCM imaging and confirmed by histopathology(Kang et al., 2010). Presence of melanophages in perilesional skin of melasma has been reported in studies based on histopathology results(Grimes et al., 2005; Kang et al., 2002).

Enhanced melanin content of the epidermis was another MPM key feature of melasma. We defined a melanin volume fraction (MVF) index corresponding to the imaged volume in each patient. We found that only epidermal melasma lesions were characterized by significantly higher MVF values compared to normal skin, while in dermal/mixed melasma patients these values were rather comparable for lesion and perilesion. We believe this might be the result of melanin migration across the basal layer into the dermis as suggested in a previous study(Torres-Álvarez et al., 2011), which leads to presence of dermal melanophages in these lesions. Studies have commonly found enhanced melanin content in melasma lesions compared to perilesional normal skin(Kang et al., 2010; Kang et al., 2002). However, the results were based on visual assessment and did not include a separate analysis of melanin content in epidermal and dermal/mixed melasma groups. An additional observation was related to the melanin distribution pattern within keratinocytes in melasma skin as compared to normal skin. In the basal layer of normal skin, melanocytes transfer melanosomes to

keratinocytes, which then align these melanosomes to form caps above their nuclei, protecting them from UV induced DNA damage. In melasma lesions, however, melanosomes in the basal cells were more often not distributed above the nuclei but appeared to be more randomly dispersed throughout the keratinocyte. These findings are consistent with the results of a previous study based on biopsy and H&E staining showing that basal keratinocytes display changes in nuclei sizes and chromatin texture in melasma lesions compared to perilesional skin(Brianezi et al., 2015).

We have also investigated the change in fibrillar structure in melasma lesions compared to adjacent normal skin. Both melasma lesions and perilesions were generally affected by elastosis, in agreement with previous reports(Hernández-Barrera et al., 2008; Sarvjot et al., 2009). Elastosis was evaluated by a dermatopathologist through visual assessment and was well correlated with a quantitative index we defined as a metric for elastosis. This metric showed an enhanced amount of elastosis in melasma compared to perilesion for most patients, regardless of the type of melasma, in accordance with previous studies based on histopathology(Hernández-Barrera et al., 2008; Sarvjot et al., 2009). While both melasma and elastosis are dependent upon UV exposure, it is unclear whether elastosis is caused by melasma (i.e. the increase in pigment content and its distribution favor the appearance of elastosis) or whether melasma and solar elastosis are independent of each other.

The changes observed in melanin distribution of basal keratinocytes and absence of melanin caps in the basal layer of the epidermis likely provide reduced photoprotection as they seemed to be associated with more pronounced dermal photodamage. Thus, 70% of lesions and perilesions showed increased elastosis associated with lack of melanin caps in the basal layer of the epidermis. Further studies are needed in order to determine whether altered distribution of melanosomes plays a role in the pathogenesis of melasma.

Although these results are limited by a modest sample size, they demonstrate the MPM potential to characterize melasma. Most notably, MPM demonstrated the ability to visualize non-invasively the signs of a prior inflammatory response, a key element in the differential diagnosis of melasma. Additionally, the technique was able to quantify the melanin amount and its distribution in the epidermal basal layer as well as dermal elastosis in melasma. The results suggest potential correlations among the melanin amount and distribution in the basal keratinocytes, dermal inflammation and photodamage. A more comprehensive study of a larger number of subjects is necessary to evaluate the ability of MPM to improve the differential diagnosis of melasma and to advance the understanding of this skin condition.

An expanded study would need to address current technical limitations related to MPM imaging, particularly the reduced field of view (FOV) and penetration depth. High penetration depth allows for a better evaluation of the melanophage population in the dermis. Penetration depth can be optimized by implementing dispersion compensation to decrease the laser pulse duration(Balu et al.,

2015a; Tang et al., 2006). Although the benefit would still be limited, the ability of MPM to visualize melanophages in melasma lesions as described in this study holds great promise. Sampling a large FOV is key for accurate diagnosis of melasma type since lesions are often non-uniform with certain features focally localized. This limitation has been recently addressed by our group in a proof-of-principle design of a bench-top MPM imaging prototype device that provides rapid scanning of large skin tissue areas, while maintaining sub-micron resolution(Balu et al., 2016).

ACKNOWLEDGEMENTS: This research was funded partially by Unilever Research and the National Institutes of Health, NIBIB Laser Microbeam and Medical Program (LAMMP, P41-EB015890), and the National Cancer Institute (1R01CA195466-01).

REFERENCES

Ardigo, M., Cameli, N., Berardesca, E., and Gonzalez, S. (2010). Characterization and evaluation of pigment distribution and response to therapy in melasma using in vivo reflectance confocal microscopy: a preliminary study. Journal of the European Academy of Dermatology and Venereology *24*, 1296-1303.

Balu, M., Kelly, K. M., Zachary, C. B., Harris, R. M., Krasieva, T. B., König, K., Durkin, A. J., and Tromberg, B. J. (2014). Distinguishing between benign and malignant melanocytic nevi by in vivo multiphoton microscopy. Cancer research *74*, 2688-2697.

Balu, M., Lentsch, G., Z., K. D., König, K., Kelly, K. M., Tromberg, B. J., and Zachary, C. B. (2017). In vivo multiphoton‐microscopy of picosecond‐laser‐induced optical breakdown in human skin. Lasers in Surgery and Medicine *49*, 555-562.

Balu, M., Mikami, H., Hou, J., Potma, E. O., and Tromberg, B. J. (2016). Rapid mesoscale multiphoton microscopy of human skin. Biomedical Optics Express *7*, 4375-4387.

Balu, M., Saytashev, I., Hou, J., Dantus, M., and Tromberg, B. J. (2015a). Sub‐40 fs, 1060‐nm Yb‐fiber laser enhances penetration depth in nonlinear optical microscopy of human skin. Journal of Biomedical Optics *20*, 120501.

Balu, M., Zachary, C. B., Harris, R. M., Krasieva, T. B., König, K., Tromberg, B. J., and Kelly, K. M. (2015b). In Vivo Multiphoton Microscopy of Basal Cell Carcinoma. JAMA dermatology *151*, 1068-1074.

Bradley, D., and Roth, G. (2007). Adaptive Thresholding using the Integral Image. Journal of Graphics Tools *12*, 13-21.

Braverman, I. M., and Fonferko, E. (1982). Studies in Cutaneous Aging: I. The Elastic Fiber Network. Journal of Investigative Dermatology *78*, 434-443.

Brianezi, G., Handel, A. C., Schmitt, J. V., Miot, L. D. B., and Miot, H. A. (2015). Changes in nuclear morphology and chromatin texture of basal keratinocytes in melasma. Journal of the European Academy of Dermatology and Venereology *29*, 809-812.

Fischer, F. F., Volkmer, B., Puschmann, S., Greinert, R., Breitbart, W., Kiefer, J., and Wepf, R. (2008). Risk estimation of skin damage due to ultrashort pulsed, focused near-infrared laser irradiation at 800 nm. SPIE).

Gilchrest, B. A., Fitzpatrick, T. B., Anderson, R. R., and Parrish, J. A. (1977). Localization of melanin pigmentation in the skin with Wood's lamp. *96*, 245-248.

Goberdhan, L. T., Colvan, L., Makino, E. T., Aguilar, C., and Mehta, R. C. (2013). Assessment of a Superficial Chemical Peel Combined With a Multimodal, Hydroquinone-Free Skin Brightener Using In Vivo Reflectance Confocal Microscopy. Journal of Drugs in Dermatology *12*, s38-s41.

Grimes, P. E., Yamada, N., and Bhawan, J. (2005). Light Microscopic, Immunohistochemical, and Ultrastructural Alterations in Patients with Melasma. American Journal of Dermatopathology *27*, 96-101.

Guitera, P., Li, L. L., Scolyer, R. A., and Menzies, S. W. (2010). Morphologic features of melanophages under in vivo reflectance confocal microscopy. *146*, 492-498.

Hernández-Barrera, R., Torres-Alvarez, B., Castanedo-Cazares, J. P., Oros-Ovalle, C., and Moncada, B. (2008). Solar elastosis and presence of mast cells as key features in the pathogenesis of melasma. *33*, 305-308.

Kang, H. Y., Bahadoran, P., Suzuki, I., Zugaj, D., Khemis, A., Passeron, T., Andres, P., and Ortonne, J.-P. (2010). In vivo reflectance confocal microscopy detects pigmentary changes in melasma at a cellular level resolution. *19*, e228-e233.

Kang, W. H., Yoon, K. H., Lee, E. S., Kim, J., Lee, K. B., Yim, H., Sohn, S., and Im, S. (2002). Melasma: histopathological characteristics in 56 Korean patients. *146*, 228-237.

Lawrence, N., Cox, S. E., and Brody, H. J. (1997). Treatment of melasma with Jessner's solution versus glycolic acid: A comparison of clinical efficacy and evaluation of the predictive ability of Wood's light examination. *36*, 589-593.

Liu, H., Lin, Y., Nie, X., Chen, S., Chen, X., Shi, B., Tian, H., Shi, Z., Yu, M., Zhang, D., et al. (2011). Histological classification of melasma with reflectance confocal microscopy: a pilot study in Chinese patients. Skin Research and Technology *17*, 398-403.

Longo, C., Pellacani, G., Tourlaki, A., Galimberti, M., and Bencini, P. L. (2014). Melasma and low-energy Q-switched laser: treatment assessment by means of in vivo confocal microscopy. Lasers in Medical Science *29*, 1159-1163.

Majdzadeh, A., Lee, A. M. D., Wang, H., Lui, H., Mclean, D. I., Crawford, R. I., Zloty, D., and Zeng, H. (2015). Real-time visualization of melanin granules in normal human skin using combined multiphoton and reflectance confocal microscopy. Photodermatology, Photoimmunology & Photomedicine *31*, 141-148.

Masters, B., So, P., Buehler, C., N., B., Jd, S., Ww, M., and Gratton, E. (2004). Mitigating thermal mechanical damage potential during two-photon dermal imaging. Journal of Biomedical Optics *9*, 1265-1270.

Ochoa, M. T., Loncaric, A., Krutzik, S. R., Becker, T. C., and Modlin, R. L. (2008). "Dermal Dendritic Cells" Comprise Two Distinct Populations: CD1+ Dendritic Cells and CD209+ Macrophages. *128*, 2225-2231.

Pellacani, G., Longo, C., Malvehy, J., and Et Al. (2008). In vivo confocal microscopic and histopathologic correlations of dermoscopic features in 202 melanocytic lesions. *144*, 1597-1608.

Pouli, D., Balu, M., Alonzo, C. A., Liu, Z., Quinn, K. P., Rius-Diaz, F., Harris, R. M., Kelly, K. M., Tromberg, B. J., and Georgakoudi, I. (2016). Imaging mitochondrial dynamics in human skin reveals depth-dependent hypoxia and malignant potential for diagnosis. Science Translational Medicine *8*, 367ra169.

Saager, R. B., Balu, M., Crosignani, V., Sharif, A., Durkin, A. J., Kelly, K. M., and Tromberg, B. J. (2015). In vivo measurements of cutaneous melanin across spatial scales: using multiphoton microscopy and spatial frequency domain spectroscopy. (Journal of Biomedical Optics.

Sarvjot, V., Sharma, S., Mishra, S., and Singh, A. (2009). Melasma: A clinicopathological study of 43 cases. Indian Journal of Pathology and Microbiology *52*, 357-359.

Sgouros , D., Pellacani, G., Katoulis, A., Rigopoulos, D., and Longo, C. (2014). Confocal Microscopy in Diagnosis and Management of Melasma: Review of Literature. Pigmentary Disorders *S1*.

Sonthalia, S., Jha, A. K., and Langar, S. (2017). Dermoscopy of Melasma. Indian Dermatology Online Journal *8*, 525-526.

Tang, S., Krasieva, T. B., Chen, Z., Tempea, G., and Tromberg, B. J. (2006). Effect of pulse duration on two-photon excited fluorescence and second harmonic generation in nonlinear optical microscopy. SPIE).

Torres-Álvarez, B., Mesa-Garza, I. G., Castanedo-Cázares, J. P., Fuentes-Ahumada, C., Oros-Ovalle, C., Navarrete-Solis, J., and Moncada, B. (2011). Histochemical and Immunohistochemical Study in Melasma: Evidence of Damage in the Basal Membrane. The American Journal of Dermatopathology *33*, 291-295.

TABLE

Table 1. Number of melanophages identified in the imaged volume for each subject

Subject	Diagnosis	Number of Melanophages in Measured Volume*		Depth of Pigment** (μm)	
		Lesion	Perilesion	Lesion	Perilesion
1	Epidermal	0	0	-	-
2	Epidermal	0	0	-	-
3	Dermal/Mixed	11	0	150	-
4	Epidermal	0	0	-	-
5	Dermal/Mixed	0	12	-	140
6	Epidermal	0	0	-	-
7	Dermal/Mixed	7	0	110	-
8	Epidermal	2	0	80	-
9	Dermal/Mixed	8	4	150	140
10	Epidermal	0	0	-	-
11	Dermal/Mixed	20	0	135	-
12	Epidermal	0	0	-	-

* Imaged volume was up to 0.6 x 0.6 x 0.15mm^3 for all sites

** Depth of pigment represents the deepest location melanophages were identified in the imaged volume

FIGURES AND LEGENDS

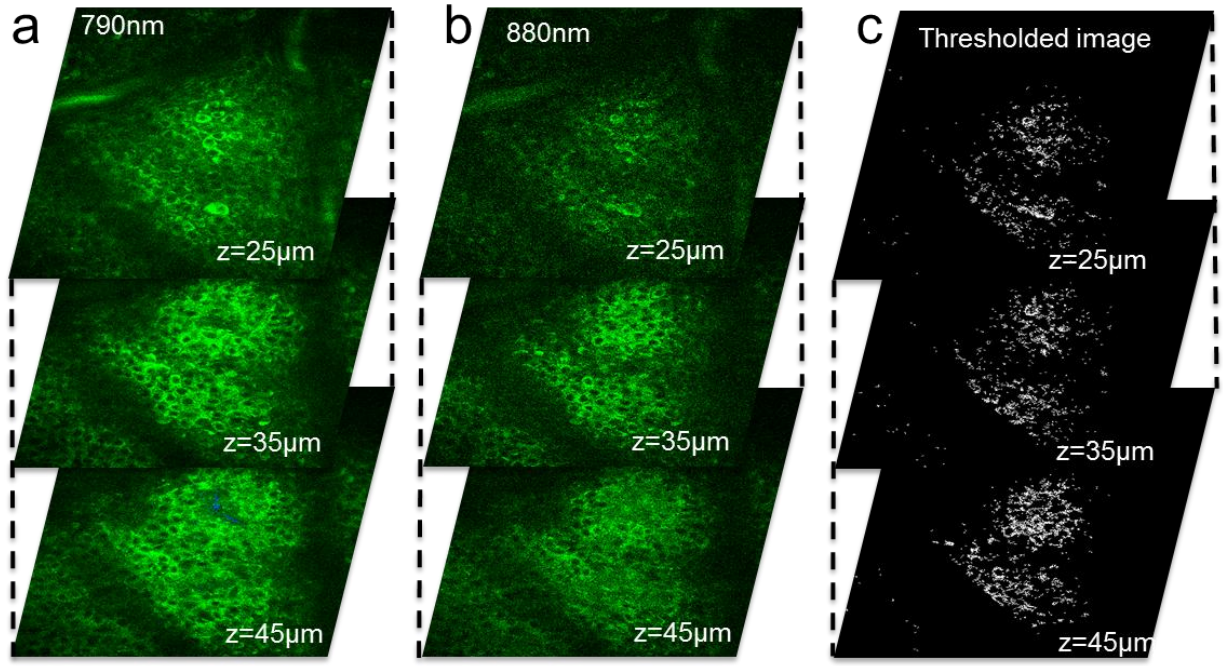

Figure 1. MPM image processing for estimating the melanin content. Stacks of TPEF images acquired at different depths at (a) 790 nm and (b) 880 nm. (c) thresholded images corresponding to the stack of TPEF images shown in (b).

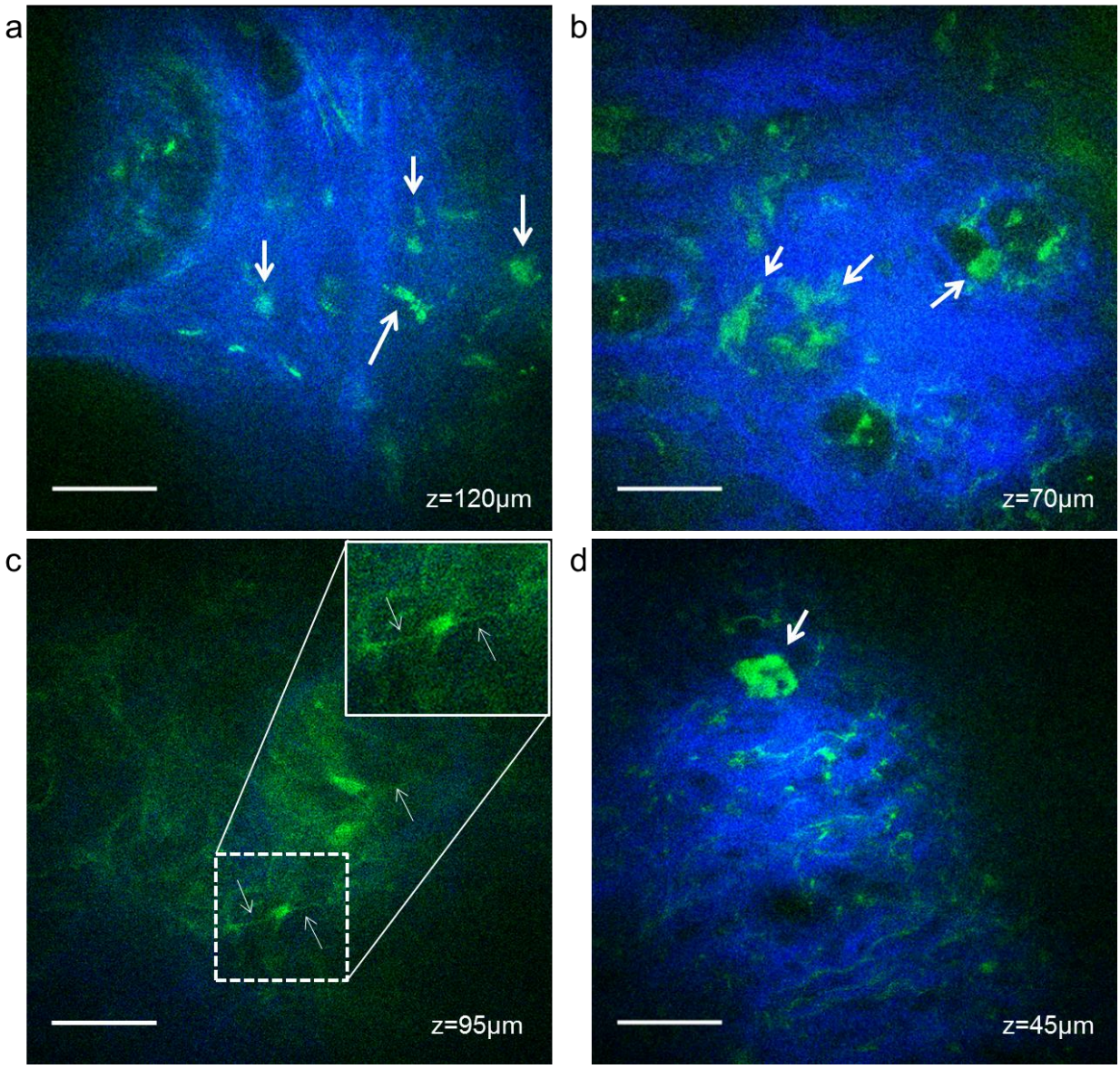

Figure 2. MPM imaging of dermal melanophages in melasma lesions- MPM images showing: (A) clusters of small dermal melanophages (arrows), (B) clusters of large dermal melanophages (arrows), (C) dendritic melanophages (arrows), and (D) individual/scattered dermal melanophages (arrow). Images in A, B, C are from subjects with dermal/mixed melasma. Image D corresponds to epidermal melasma. Collagen and elastin fibers are visualized in dermis by their SHG (blue) and TPEF (green) signals, respectively. 'z' represents depth in all MPM images. Scale bar is 40 µm.

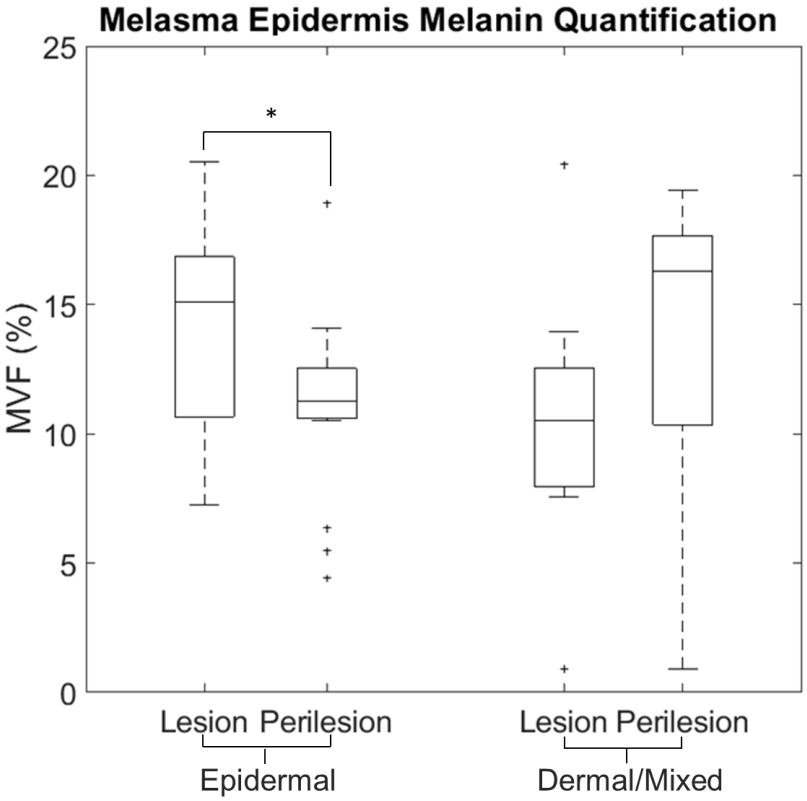

Figure 3. Distribution of the mean MVF values – The distribution of the mean MVF values measured in all lesions diagnosed as epidermal melasma (*p=0.03) and dermal/mixed melasma (p=0.32) and in corresponding perilesional skin.

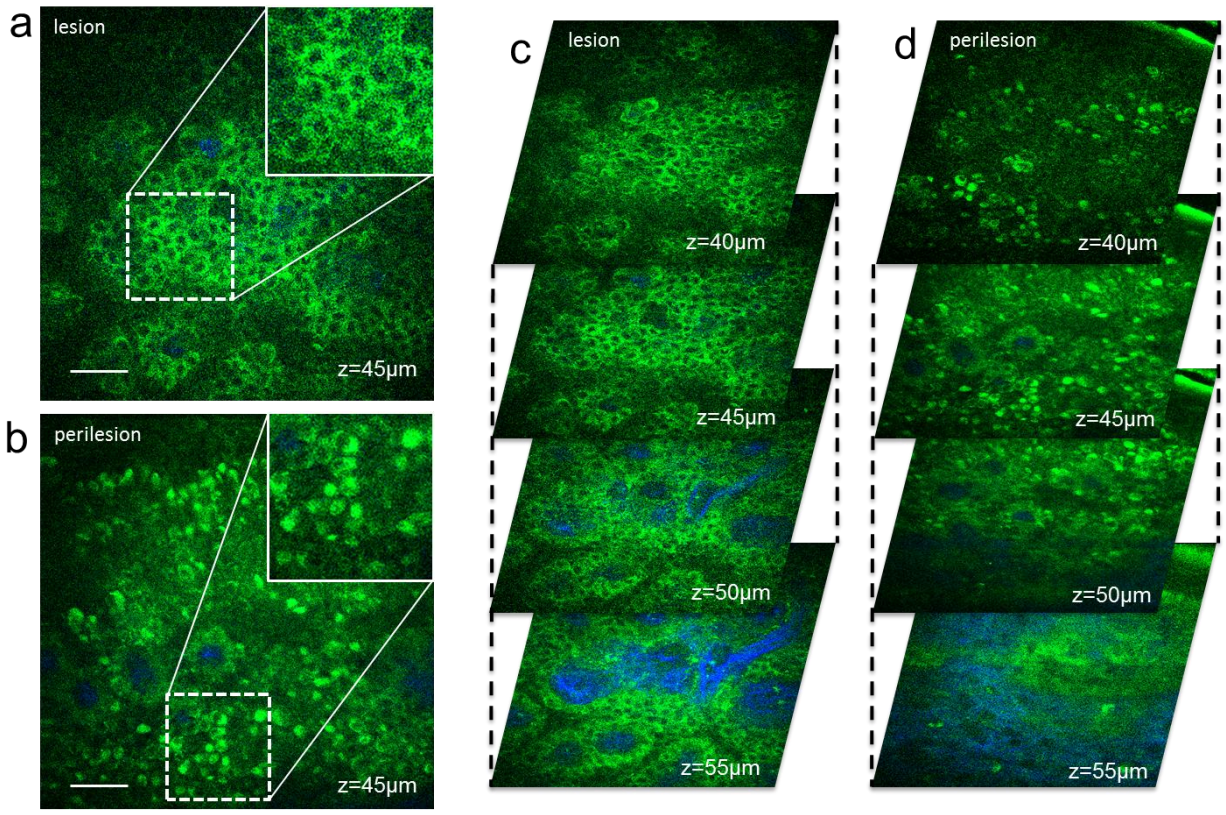

Figure 4. MPM imaging of epidermal melanin distribution in melasma lesion and perilesion- MPM images showing: (a) melasma lesional skin, with pigment distribution localized mainly towards the cellular membrane, and (b) perilesional skin, with pigment distribution localized mainly towards the nuclear membrane (melanin caps). The insets in (a) and (b) show a close-up of the melanin distribution in the lesion and perilesion keratinocytes. These images were selected from the corresponding stacks acquired at different depths as shown in (c) and (d). MPM images are from a subject with dermal/mixed melasma. 'z' represents depth in all MPM images. Scale bar is 40 µm.

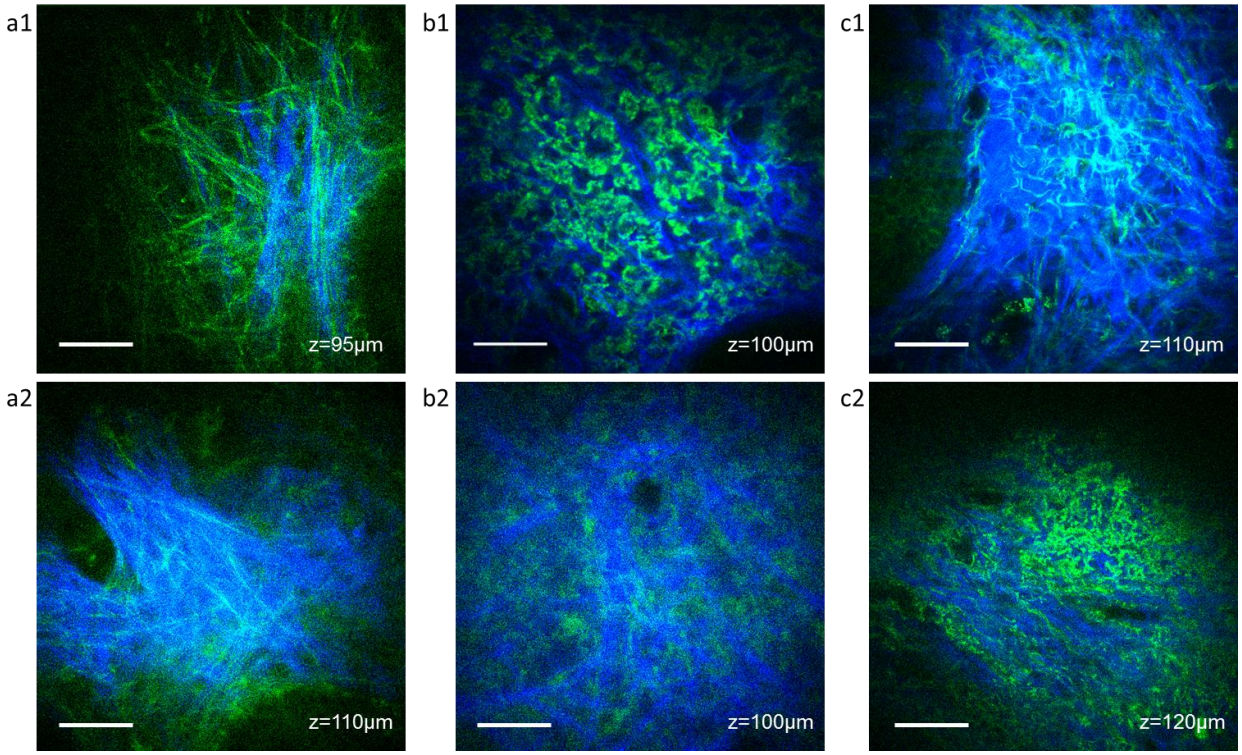

Figure 5. MPM imaging of elastosis in melasma lesion and perilesional skin – MPM images of the dermis in the lesion (A1, B1, C1) showing severe elastosis with overproduction of normal elastin fibers (A1, C1), and abnormal elastin fibers (B1); MPM images of the dermis in the corresponding perilesion (A2, B2, C2) showing: moderate elastosis (A2), mild elastosis (B2), and moderate elastosis with overproduction of abnormal elastosis fibers (C2). Collagen and elastin fibers are visualized in dermis by their SHG (blue) and TPEF (green) signals, respectively. 'z' represents depth in all MPM images. Scale bar is 40 µm.

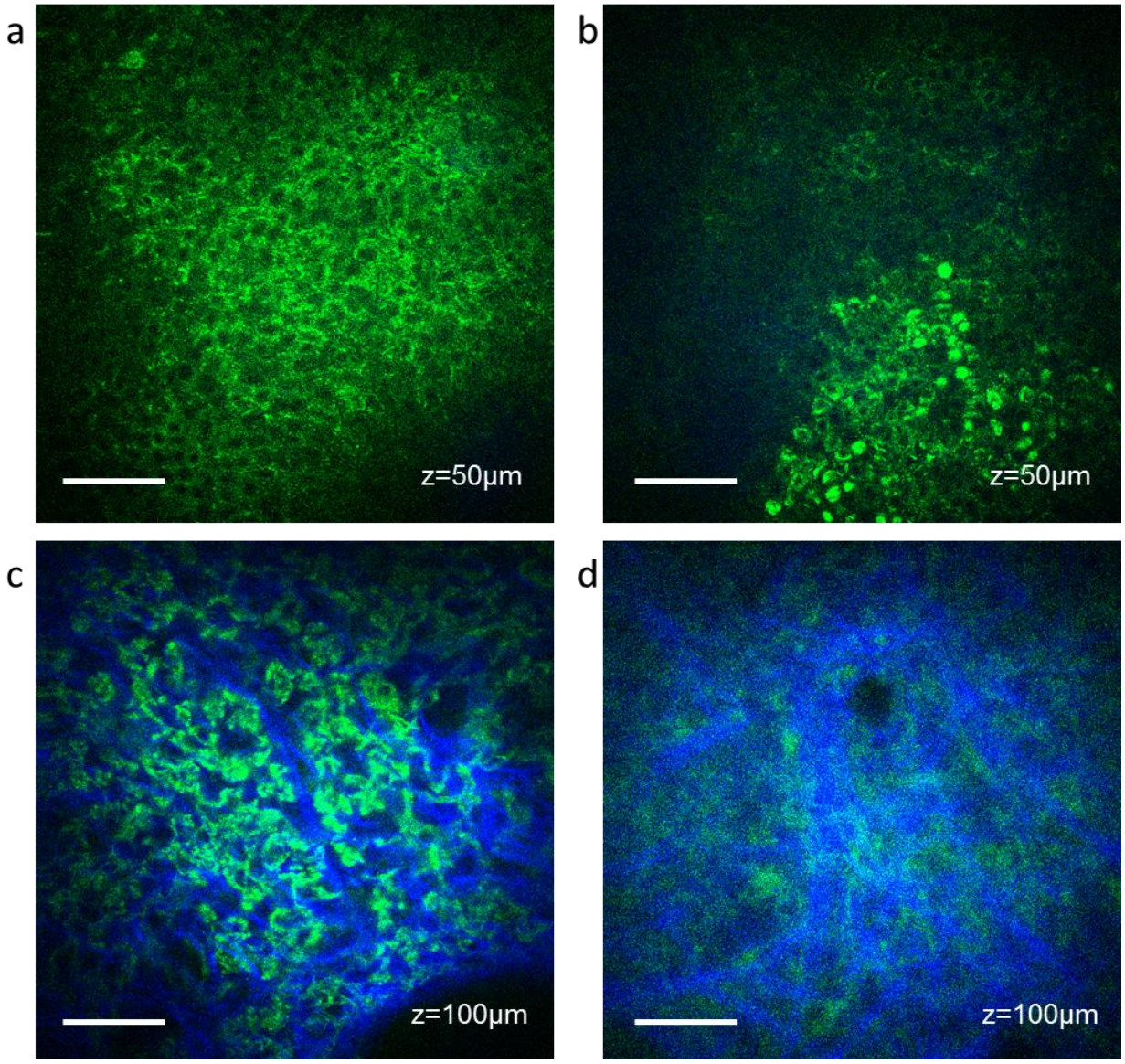

Figure 6. Representative MPM images of epidermal pigment distribution in the basal layer vs. elastosis severity in melasma lesion and perilesional skin – MPM image of the epidermis in the lesion (A) showing an epidermal pigment distribution localized towards the cellular membrane, and perilesion (B) showing an epidermal pigment distribution localized towards the nuclear membrane (melanin caps); MPM images of the dermis in the lesion (C) showing severe elastosis with overproduction of abnormal elastosis fibers, and perilesion (D) showing mild elastosis. Collagen and elastin fibers are visualized in dermis by their SHG (blue) and TPEF (green) signals, respectively. 'z' represents depth in all MPM images. Scale bar is 40 μm.

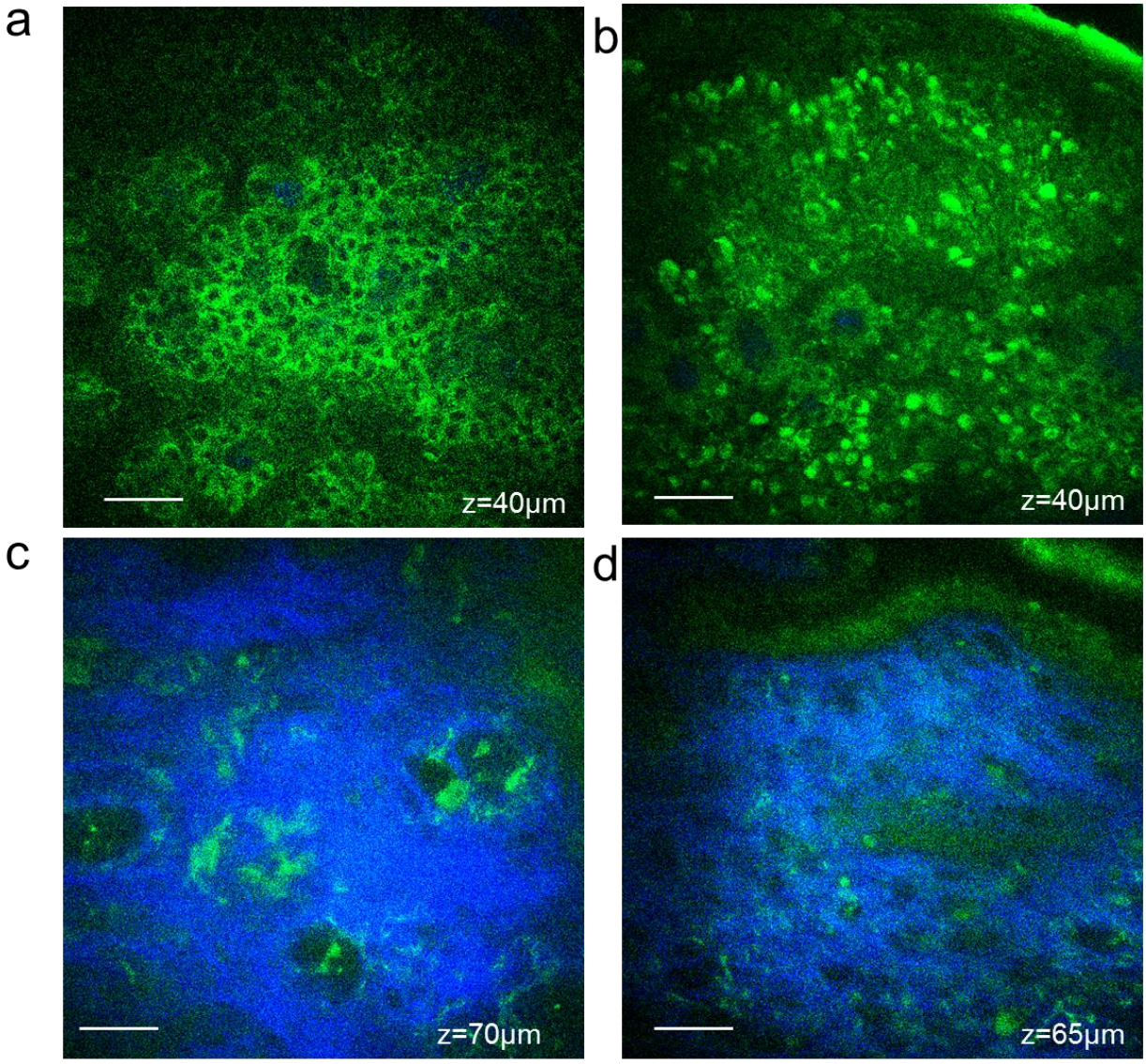

Figure 7. Representative MPM images of epidermal pigment distribution in the basal layer vs. presence of dermal melanophages in melasma lesion and perilesional skin – MPM image of the epidermis in the lesion (A), showing an epidermal pigment distribution localized towards the cellular membrane, and perilesion (B), showing an epidermal pigment distribution localized towards the nuclear membrane (melanin caps); MPM images of the dermis in the lesion (C), showing clusters of dermal melanophages, and perilesion (D), showing no dermal melanophages. Collagen and elastin fibers are visualized in dermis by their SHG (blue) and TPEF (green) signals, respectively. 'z' represents depth in all MPM images. Scale bar is 40 µm.